Scientific Reports

https://doi.org/10.1038/s41598-026-41417-2

Article in Press

Traffic pattern-adaptive channel allocation in cognitive radio networks via multi-scale windowing

Received: 19 December 2025

Accepted: 19 February 2026

Published online: 22 February 2026

Cite this article as: Min Z., Ziru W., Jinyuan B. *et al.* Traffic pattern-adaptive channel allocation in cognitive radio networks via multi-scale windowing. *Sci Rep* (2026). https://doi.org/10.1038/s41598-026-41417-2

Zhang Min, Wu Ziru, Bai Jinyuan & Zhang Bo

Traffic Pattern-Adaptive Channel Allocation in Cognitive Radio Networks via Multi-Scale Windowing

Zhang Min[1], **Wu Ziru**[1,*], **Bai Jinyuan**[1], **and Zhang Bo**[1]

[1]School of Electronics and Information Engineering, Liaoning Technical University, Huludao City 125105, China
[*]corresponding.author:E-mail:1394922986@qq.com

ABSTRACT

A major challenge in enhancing the performance of multi-user cognitive radio networks lies in accurately characterizing the dynamic service arrivals of secondary users (SUs) for optimal spectrum utilization. To enhance protocol adaptability in complex traffic environments, this paper proposes a Traffic Pattern-Adaptive Allocation (TPA) protocol. Integrating Markov modeling with queueing theory, TPA employs multi-scale windows to concurrently measure SU traffic arrivals. By incorporating an adaptive window weight adjustment mechanism, the protocol achieves a granular characterization of the SU arrival process. Furthermore, it constructs a Probability Allocation Vector to dynamically map traffic states to channel allocation strategies, enabling automatic adjustment of resource policies in response to traffic fluctuations. Experimental results demonstrate that, compared to the Maximum Throughput Allocation protocol, TPA delivers higher throughput and lower packet rejection rates under complex traffic dynamics. This approach thus offers a robust solution for addressing the stochastic nature of user demands in next-generation cognitive radio systems.

Keywords: Cognitive Radio, Spectrum Allocation, Probability Allocation Vector, Maximum Throughput Allocation Protocol, TPA Protocol

1 Introduction

With the continuous growth of wireless communication traffic and increasing service demands, the contradiction between scarce spectrum resources and low utilization rates has become increasingly pronounced[1–3]. The traditional fixed spectrum licensing model has difficulty accommodating these demands. Under this framework, PUs hold absolute priority rights over licensed bands, while Secondary Users (SUs) can only access residual spectrum opportunistically when Primary Users (PUs) are idle[4–6].However, PU services often exhibit random and sporadic characteristics. This results in long-term spectrum underutilization and consequently low overall efficiency. To resolve this contradiction, Mitola and Maguire introduced the paradigm of Cognitive Radio (CR) in 1999[7]. CR fundamentally transforms wireless nodes from static transceivers into intelligent agents capable of sensing their electromagnetic environment. By adopting an interweave dynamic spectrum access strategy, Secondary Users (SUs) can opportunistically identify and exploit these spectrum holes without causing harmful interference to PUs.This has become a key technological pathway for enhancing spectrum utilization[8–10].

Despite the theoretical maturity of Cognitive Radio concepts, the combined effects of PU occupancy behavior, the time-varying characteristics of wireless channels (such as rapid fading and SNR fluctuations), and the dynamic arrival of SU services in practical CRNs make the design of channel resource management and allocation strategies highly complex[11–14]. To manage this complexity, researchers have extensively employed queueing theory to derive performance metrics such as throughput, delay, and packet rejection rates.Queueing models provide the mathematical rigor necessary to characterize the interactions between random service interruptions and data accumulation[15–20].For instance, Wang et al.[21]developed a foundational queueing framework tailored for CRNs, allowing for the quantitative assessment of delay distributions. Building on this, Adem and Hamdaoui[22]integrated Discrete-Time Markov Chains to model PU activity as a two-state process coupled with SU buffer dynamics, yielding closed-form expressions for service latency. Similarly, Zhao and Sadler[23] proposed the classic dynamic spectrum access model, establishing the theoretical groundwork for PU activity modelling and SU opportunistic access in CR systems.However, their work assumes SU traffic arrivals follow a Poisson process, which fails to capture the bursty traffic patterns commonly observed in real-world networks[24]. Liu et al.[25] constructed a joint Markov chain that integrates PU activity, channel state, and SU buffer behavior, significantly improving the accuracy of system dynamic modelling. Nevertheless, they typically rely on fixed statistical windows for traffic estimation. Fixed-window approaches are inherently reactive: a window that is too long fails to detect sudden bursts in time to reallocate resources, while a window that is too short introduces jitter and instability into the allocation decision.

In the domain of resource scheduling, the Maximum throughput channel allocation protocol proposed by Wang et al.[26] theoretically improves the system throughput of multi-user, multi-channel cognitive radio networks by constructing an allocation

probability matrix and selecting long-term optimal allocation strategies based on queueing models[27,28]. However, this method emphasizes long-term statistical optimization and does not sufficiently address the bursty and time-varying characteristics of SU traffic over short timescales. Jia et al.[29] adopted an enhanced bipartite matching algorithm for optimal channel allocation, achieving improvements in channel utilization. Nevertheless, their scheduling approach remains primarily rooted in static statistical information and lacks a traffic-driven mechanism.Despite these advances, existing research still presents two notable limitations. First, although SU services typically exhibit multi-scale, time-varying behaviour, most current models assume Poisson-based arrivals or rely on fixed single-window statistics, which cannot accurately reflect the inherent complexity of real service patterns[30]. Second, many studies apply one-dimensional modelling—either for PU activity or SU buffer states—while overlooking the joint interaction among PU activity, channel condition, and SU buffer dynamics. This simplification reduces analytical accuracy and constrains the representation of real-world dynamics[31–34]. Moreover, service arrival characteristics have not been effectively incorporated into channel allocation strategies. As a result, existing protocols are prone to issues such as reduced throughput, buffer overflows, and higher rejection rates under bursty or complex traffic scenarios[35–37].

To address the aforementioned issues, this paper proposes the Traffic Pattern-Adaptive Allocation (TPA) adaptive window channel allocation protocol and develops a comprehensive performance analysis framework based on queueing theory and Markov models. The framework utilizes multi-scale adaptive windows to refine the modelling of SU data arrival processes. It then maps service states to the channel allocation protocol through a Probability Allocation Vector (PAV), allowing the protocol to maintain stable performance under both steady-state and bursty traffic conditions. This approach effectively bridges the gap between time-varying service modelling and real-time channel allocation present in existing research, providing CR systems with a more precise and robust resource management methodology.

The main contributions of this paper are as follows:

- Development of the TPA Protocol:We introduce a novel adaptive window channel allocation protocol driven by PAV. By integrating multi-scale parallel window statistics with adaptive weight adjustment, the protocol accurately identifies traffic states. These states are modeled via a Markovian transition matrix, allowing the allocation logic to preemptively adapt to traffic evolution, thereby enhancing spectrum utilization efficiency.

- Unified Performance Analysis Framework:We present a comprehensive queueing-theoretic evaluation framework for multi-user, multi-channel CR systems. Unlike previous studies that decouple system components, we establish a system-level Markov state space that jointly integrates PU activity, channel conditions, and SU buffer states. This holistic model enables the rigorous derivation of key performance indicators —including throughput and packet rejection rates,providing an objective benchmark for comparing TPA against conventional MTA protocols under dynamic traffic conditions.

The remainder of this article is structured as follows:

Section 2 outlines the system model and the associated assumptions, encompassing both PU and SU models. In Section 3, a queueing-theoretic analysis is conducted through a discrete-time Markov framework to characterize the dynamics of the system states. Based on this model, the state transition matrix and steady-state distribution are derived, which are subsequently used to evaluate key performance metrics. Section 4 details the design principles and implementation procedures of the MTA and TPA protocols. Section 5 presents numerical simulation results accompanied by a comprehensive analysis. Finally, Section 6 primarily serves as a summary of the paper and an outlook for the future.

2 System Model and Assumptions

2.1 Network Model

The cognitive radio network considered in this study consists of multiple SUs and PU channels, with its overall architecture depicted in Figure 1. The system comprises M SUs, N PU channels, two base stations dedicated to serving PUs and SUs, respectively, and a centralized management center. The management center is responsible for monitoring spectrum opportunities and the occupancy status of all channels within the network. Based on real-time observations, it dynamically allocates available channels that are not currently occupied by PUs to SUs, while concurrently gathering essential information necessary for system operation. The network operates in accordance with cognitive radio spectrum sharing principles: PUs retain the highest priority for licensed bands, where as SUs are permitted to access idle spectrum only under the condition that they do not cause interference to PUs.

This study examines the uplink data transmission process, assuming that all information within the network is conveyed as discrete data packets. For spectrum access, the SU system operates in an overlay mode, sharing the same frequency band with the PU system. Specifically, uplink transmission by SUs is permitted only when the corresponding PU channel is idle; upon detecting PU activity or the reoccupation of the channel, the SU must immediately suspend its transmission. Additionally, each SU terminal is equipped with a finite-capacity buffer queue to store data packets awaiting transmission.

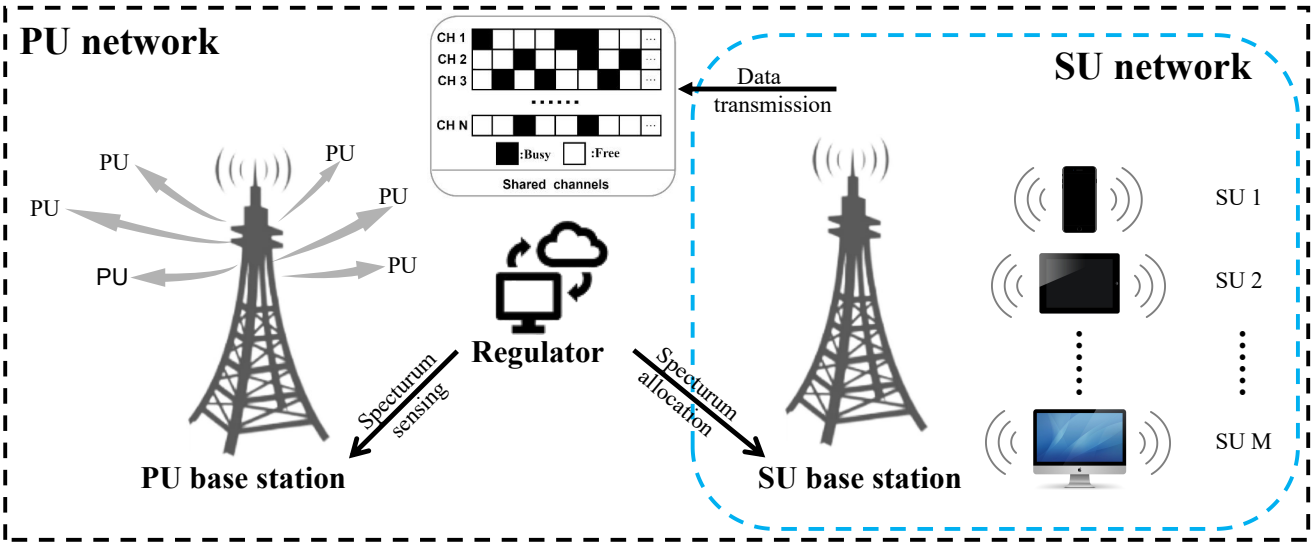

Figure 1. Network model

2.2 PU Activity Model

In CR systems, the ability of a SU to access a channel for data transmission is contingent upon the occupancy status of that channel by a PU. Therefore, constructing an accurate model of PU activity is essential. In this study, a discrete-time Markov chain is employed to characterize the occupancy state of each PU channel, modeling each channel as a two-state random process: Busy and Free.

For the i-th PU channel, its activity state at time slot t is denoted as $s_i(t) \in 0, 1$, where $s_i(t) = 1$ indicates that the channel is occupied by the PU during time slot t, and $s_i(t) = 0$ indicates that the channel is idle, allowing potential access by SUs.

Under this framework, the state transitions of the PU channel between consecutive time slots are described by a first-order Markov chain, with the corresponding state transition matrix defined as:

$$P_s^i = \begin{bmatrix} P_{b\to b}^i & P_{b\to f}^i \\ P_{f\to b}^i & P_{f\to f}^i \end{bmatrix} \tag{1}$$

where, $P_{b\to b}^i + P_{b\to f}^i = P_{f\to b}^i + P_{f\to f}^i = 1$, $P_{b/f\to b/f}^i$ denotes the probability that the i-th PU channel transitions from Busy(Free) to Busy(Free) between time slot t and time slot (t+1).

2.3 SU Model

2.3.1 Data Arrival Model

In CR systems, the stochastic nature of PU activity induces significant fluctuations in the availability of spectrum resources, leading to time-varying characteristics in the actual data services of SUs. Consequently, statistical methods are often required to model SU data arrival patterns.

Compared to conventional wireless communication systems, SU traffic exhibits more pronounced variability, particularly when PUs occupy channels for extended periods or frequently switch between spectrum bands. Under such conditions, classical Bernoulli or fixed-probability arrival models often fail to accurately capture the burstiness and temporal instability of SU traffic. To better reflect the diversity and phased characteristics of SU data arrivals, this study categorizes SU traffic into two states: the Normal Service State and the Burst Service State. Each state is associated with an independent packet arrival probability distribution, characterizing the expected number of packets arriving under that state.

To determine whether the current arrival behavior corresponds to the Normal or Burst Service State, the system aggregates traffic volumes across multiple time windows of varying lengths and applies a weighted fusion process to estimate the current load intensity. If the resulting average falls below a predefined threshold, the system classifies the traffic as Normal Service State; otherwise, it is identified as Burst Service State.The traffic classification threshold is determined according to the statistical characteristics of SU packet arrivals observed over a sufficiently long time horizon. These include metrics such as the average packet arrival rate.

In determining the traffic state of SU in CR, the arrival behavior of the SU's traffic data is first modelled as a discrete-time sequence. The continuous time axis is partitioned into discrete time units of equal granularity (e.g. time slots), constructing a

binary indicator sequence $X = \{x_t \mid t \in [1,T]\}$ (where T denotes the number of time units corresponding to the observation duration).Here,$x_t = 1$ indicates data arrival at the SU during the t-th time unit (active service period), while $x_t = 0$ signifies no data arrival (idle service period). To extract effective resource units where the SU can transmit continuously without interference, consecutive segments in the sequence satisfying $x_t = 1$ and separated by idle periods are defined as 'service window'. Each window corresponds to an independent PU idle event (spectrum opportunities). The collection of all independent windows forms the set $\Omega \in \{1,2,3,\cdots,n\}$ (where n is the total number of windows). The length of the i-th window is quantified by boundary indices: The start index p_i satisfies $x_{p_i} = 1$ and $x_{p_{i-1}} = 0$, while the end index q_i satisfies $x_{q_i} = 1$ and $x_{q_{i-1}} = 0$.The length formula is $x_i = q_i - p_i + 1$.

To describe the allocation of arrival windows for data in different time slots, a set of windows $\Omega \in \{1,2,3,\cdots,n\}$ is introduced. The weight values for each window are assigned according to the window length:

$$\omega_i = \frac{x_i}{x_1 + x_2 + \cdots + x_n} \tag{2}$$

Here, ω_i denotes the weight value of the i-th window, and x_i denotes the length of the i-th window. The states N and B are introduced to represent the Normal Service State and the Burst Service State data arrival models, respectively. The packet arrival probability for the Normal Service State is denoted as $\vec{\sigma}_N^i = \{\sigma_N^i(0), \sigma_N^i(1), \cdots, \sigma_N^i(q_{\max})\}$, while that for the Burst Service State is denoted as $\vec{\sigma}_B^i = \{\sigma_B^i(0), \sigma_B^i(1), \cdots, \sigma_B^i(q_{\max})\}$. $\sigma_N^i(k)$ and $\sigma_B^i(k)$ denote the probability of k packets arriving in the i-th window during normal and Burst Service State respectively. The packet arrival state transition matrix for the i-th window is expressed as:

$$a_{rr}^i = \begin{bmatrix} \sigma_{N\to N}^i & \sigma_{N\to B}^i \\ \sigma_{B\to N}^i & \sigma_{B\to B}^i \end{bmatrix} \tag{3}$$

The packet arrival probability and state transition matrix for each window are weighted and aggregated to derive the overall packet arrival probability ($\vec{p}_N$, $\vec{p}_B$) and packet state transition matrix A_{rr}:

$$\vec{p}_N = \sum_i \omega_i \sigma_N^i \tag{4}$$

$$\vec{p}_B = \sum_i \omega_i \sigma_B^i \tag{5}$$

$$A_{rr} = \sum_i \omega_i a_{rr}^i \tag{6}$$

Based on the state transition matrix A_{rr}, the steady-state probability $\pi_j = [\pi_N^j, \pi_B^j]$ is obtained. For the j-th SU, the total data arrival probability distribution is expressed as $\vec{p}_j = \vec{p}_N^j \pi_N^j + \vec{p}_B^j \pi_B^j$.

2.3.2 Data Transmission Model

In the CRN of this study, the SU transmits uplink data using a time-slotted framework synchronized with the PU system. To characterize the SU's data transmission capability across different PU channels, this study employs the channel condition state (receiver signal-to-noise ratio) as a metric reflecting its transmission capability.The impact of wireless propagation effects such as path loss, shadowing, and fading is implicitly captured through the SNR state transitions.

For the i-th PU channel, the SNR range at the SU receiver is divided into N_{SNR}^i discrete intervals, thereby constructing the channel condition state set as: $\vartheta_i \in \{1,2,\cdots,N_{SNR}^i\}$. Considering the randomness of channel variations over time, this paper employs a finite-state Markov chain to model the channel condition states, with its transition matrix expressed as:

$$P_\vartheta^i = \left[p_{x\to y}^{(i)}\right] = \begin{bmatrix} p_{0\to 0}^i & \cdots & p_{0\to N_{SNR}^i}^i \\ \vdots & \ddots & \vdots \\ p_{N_{SNR}^i\to 0}^i & \cdots & p_{N_{SNR}^i\to N_{SNR}^i}^i \end{bmatrix} \tag{7}$$

Here, $p_{x\to y}^{(i)}$ denotes the probability that channel i transitions from the current time slot state x to the next time slot state y.

To maximize spectrum utilization, the SU system employs an adaptive modulation and coding (AMC) scheme that selects the optimal transmission mode based on current channel conditions. The AMC scheme enables SUs to achieve differentiated data rates under varying channel states, enhancing overall spectrum efficiency. The system management center obtains real-time

status of PU activity through spectrum sensing and allocates idle channels to SUs for data transmission according to the current condition of PU channels. Regarding resource allocation rules, the system stipulates that each PU channel can be assigned to only one SU within the same time slot, while a single SU can simultaneously access multiple available PU channels for parallel transmission. To further analyze different channel allocation strategies, this study introduces PAV to quantitatively represent various channel allocation protocols.

After acquiring PU channel resources, the SU transmits data based on the assigned channel and its conditional state. Suppose the j-th SU transmits data using a channel with conditional state n. The number of data packets it can transmit within a unit time slot follows a discrete probability distribution:

$$\vec{\sigma}_{i,n}(m) = [\sigma_{i,n}(0), \sigma_{i,n}(1), \cdots, \sigma_{i,n}(k)] \tag{8}$$

Here, $\sigma_{i,n}(m)$ denotes the probability of transmitting m data packets under the given channel condition, where k represents the maximum number of packets that can be transmitted in that time slot.

2.3.3 Probability Assignment Vector (PAV)

In CRN, due to the diverse design objectives of different channel allocation protocols, a unified mathematical framework is required to facilitate performance comparisons among these protocols. To this end, this paper proposes an $(M+1)^N$ dimensional PAV to describe the probability distribution of allocation outcomes for different channel allocation protocols. The mathematical definition of the PAV is as follows:

$$\vec{V} = (V_1, V_2, V_3, \cdots, V_{(M+1)^N}) \tag{9}$$

Here, V_i denotes the probability that the i-th channel assignment outcome occurs among all $(M+1)^N$ possible outcomes, and the sum of all V_i equals 1.

The specific allocation result for each channel can be represented by vector $\vec{\gamma}_i = [\gamma_i^1, \gamma_i^2, \gamma_i^3, \cdots, \gamma_i^N]$, where $\gamma_i^n \in \{x\colon 0 \le x \le M, x \in \mathbb{N}\}$ denotes the allocation status of the nth channel. When $\gamma_i^n = x\ (x \neq 0)$, it indicates that the nth channel is allocated to the x-th SU. When $\gamma_i^n = 0$, it indicates that the nth channel is occupied by a PU, rendering it unavailable to SUs.

It follows that when the number of channels N and the number of SUs M in a system are fixed, all possible channel allocation outcomes can be transformed into probability-based PAVs. This also implies that different channel allocation protocols can be converted into corresponding PAVs and adapted to the unified performance analysis framework proposed in this paper.

3 Queuing Theory Analysis Framework Based on Markov Models

In evaluating the performance of the channel allocation protocol, this study first established a queue structure under discrete time slots for each SU to describe its data arrival and transmission process. Subsequently, a discrete-time Markov model is employed to characterize changes in system states, which primarily encompassed PU activity state, channel condition state, and SU buffer state. Based on the Markov model, the system state transition probability matrix was derived, and the steady-state distribution was calculated from this. Using the steady-state results, two key performance indicators—throughput and packet rejection rate—were further obtained.

3.1 System State

In the Markov model, the system state primarily consists of PU Activity State, Channel Condition State, and SU Buffer State.

PU Activity State:

There are N PU channels in this research system,each of which can be in either the "Free" or "Busy" state at any given time slot. By introducing an N-dimensional vector $\vec{s} = (s_1, s_2, s_3, \cdots, s_N)$ to describe the real-time activity state of all PU channels, Each component s_i $(i \in \{1,2,3,\cdots,N\})$ takes only two discrete values, For $s_i = 1$ and $s_i = 0$ respectively, all possible PU activity state vectors form the PU activity state set S. The number of possible activity states is 2^N.

$$\vec{s} \in S = \{(s_1, s_2, \cdots, s_N) \mid s_i \in \{0,1\},\ i \in \{1,2,\cdots,N\}\} \tag{10}$$

Channel Condition State:

In the CR system, channel availability depends not only on whether the PU is occupied but also on random fluctuations in the wireless propagation environment, such as path loss, shadowing, and SNR. To describe the impact of the channel on SU transmission capability, this study employs a "signal-to-noise ratio discretization" approach to model channel conditions. Define the channel condition vector as $\vec{\vartheta} = (\vartheta_1, \vartheta_2, \vartheta_3, \cdots, \vartheta_N)$,where $\vartheta_n \in \{1,2,3,\cdots,N_{SNR}^n\}$ denotes the discretized signal-to-noise ratio level of the nth channel. N_{SNR}^n denotes the number of SNR states defined for this channel.

Therefore, the channel condition Status space can be represented as:

$$\vec{\vartheta} \in \Theta = \{(\vartheta_1, \vartheta_2, \cdots, \vartheta_N) \mid \vartheta_n \in \{1,2,\cdots,N_{SNR}^n\},\ n \in \{1,2,\cdots,N\}\ \} \tag{11}$$

SU Buffer State:

In dynamic spectrum environments, data arrivals at the SU are typically bursty and unpredictable, and caching capabilities vary among different SUs. Therefore, a queueing model is required to describe the caching state of the SU.

Suppose the system has M SU users. Define the SU buffer state vector as:

$$\vec{\xi} = (\xi_1, \xi_2, \xi_3, \cdots, \xi_M) \tag{12}$$

Here, ξ_i denotes the number of data packets stored by the i-th SU in the current time slot. $\xi_i \in \{0, 1, 2, \cdots, L_i\}$, where L_i denotes the maximum capacity of the i-th SU buffer.

Therefore, the SU buffer State space can be represented as:

$$\vec{\xi} \in \Xi = \{(\xi_1, \xi_2, \cdots, \xi_M) \mid \xi_i \in \{0, 1, 2, \cdots, L_i\},\ i \in \{1, 2, 3, \cdots, M\}\ \} \tag{13}$$

The combined modeling of PU activity state, channel condition state, and SU buffer state constitutes the overall system state. The aggregate state of the system at any given time t is expressed as:

$$\Gamma(t) = (s(t), \vartheta(t), \xi(t)) \tag{14}$$

Therefore, the system State space is defined as:

$$\Gamma = \{(s, \vartheta, \xi) \mid s \in S, \vartheta \in \Theta,\ \xi \in \Xi\ \} \tag{15}$$

3.2 System State Probability Transition Matrix

PU Activity Joint State Transition Matrix:

Based on the transition probabilities of the PU states for each channel, construct the corresponding PU activity state transition matrix, denoted as P_S.

$$P_S = P_S^1 \otimes P_S^2 \otimes P_S^3 \otimes \cdots \otimes P_S^N \tag{16}$$

Channel Union State Transition Matrix:

For the n-th channel, its SNR is divided into N_{SNR}^n levels. By combining the state transition probabilities of all channels' SNRs, the joint channel transition matrix P_Θ is obtained.

$$P_\Theta = P_\Theta^1 \otimes P_\Theta^2 \otimes P_\Theta^3 \otimes \cdots \otimes P_\Theta^N \tag{17}$$

SU Buffer Joint State Transition Matrix:

The SU buffer is used to store data awaiting transmission, and its state is influenced by packet arrival and packet transmission processes. Suppose the system has M SUs, where the buffer capacity of the i-th SU is L_i, The current SU buffer state is ξ_i, the packet arrival probability is $\vec{p}_i$, and the current channel condition states are$\vec{\sigma}_{(i,1)}, \vec{\sigma}_{(i,2)}, \vec{\sigma}_{(i,3)}, \cdots, \vec{\sigma}_{(i,N_{SNR}^i)}$, The probability vector for packet arrival and transmission within a time slot for the i-th SU is represented as:

$$\vec{\psi}_i = \mathrm{Conv}\left(\xi_i, \vec{p}_i, \vec{\sigma}_{(i,1)}, \vec{\sigma}_{(i,2)}, \vec{\sigma}_{(i,3)}, \cdots, \vec{\sigma}_{(i,N_{SNR}^i)}\right) \tag{18}$$

Conv represents the convolution operation, which combines the probability distributions of three independent processes—cache state, packet arrival, and packet transmission—to derive the probability vector for cache state transitions.

Additionally, the channel allocation protocol also influences the transition of SU cache states. Therefore, when deriving the transition probability matrix for SU cache states, the impact of PAV must be taken into account.

When the PU activity state is $\vec{s}_k = (s_1, s_2, s_3, \cdots, s_N)_k$, where k denotes the k-th PU activity state and $k \in \{0, 1, 2, \cdots, 2^N\}$. The vector $\vec{w}_k = (w_k^1, w_k^2, w_k^3, \cdots, w_k^N)$ represents the channel occupancy of the SU under the state of the PU, When $w_k^i = 0$, it indicates that the i-th channel is occupied by a PU. When $w_k^i = x$, it indicates that the channel is allocated for use by the x-th SU, where $x \in \{1, 2, 3, \cdots, M\}$. From this, the sum φ_a^k of all possible channel allocation probabilities under the PU activity state $\vec{s}_k$ can be calculated, expressed as follows:

$$\varphi_a^k = \sum_{k=1}^{2^N} \sum_{i=1}^{N} \sum_{n=1}^{(M+1)^N} \sum_{w_k^i = \gamma_n^i} V_n \tag{19}$$

The state transition probability vector for the i-th SU buffer can thus be obtained as:

$$\vec{p}_{\xi}^{\,i} = \sum_{k=1}^{2^N} \sum_{w_k^i \neq 0} \varphi_a^k \cdot \vec{\psi}_i \tag{20}$$

When the cache state of all SUs in the system at a given moment is $\vec{\xi}_j = (\xi_1, \xi_2, \xi_3, \cdots, \xi_N)_j$, the joint transition probability of the overall buffer is

$$\vec{p}_{\Xi}^{\,j} = \vec{p}_{\xi}^{\,1} \otimes \vec{p}_{\xi}^{\,2} \otimes \vec{p}_{\xi}^{\,3} \otimes \cdots \otimes \vec{p}_{\xi}^{\,M} \tag{21}$$

By integrating the SU cache states, the state transition matrix for the entire SU buffer is obtained as follows:

$$P_{\Xi} = \begin{bmatrix} p_{0,0}^{\xi} & \cdots & p_{0,r_\xi}^{\xi} \\ \vdots & \ddots & \vdots \\ p_{r_\xi,0}^{\xi} & \cdots & p_{r_\xi,r_\xi}^{\xi} \end{bmatrix} \tag{22}$$

Here, $r_\xi = \prod_{i=1}^{M} L_i$ denotes the total number of all possible combinations of SU buffer states.

By combining the PU activity state transition matrix, the channel condition state transition matrix, and the aforementioned cache state transition matrix, a complete system state transition matrix χ can be constructed. The total number of possible system states is $r_s = 2^N \prod_{i=1}^{M} L_i \prod_{n=1}^{N} N_{SNR}^n$.

$$\chi = P_S \otimes P_\Theta \otimes P_\Xi = \begin{bmatrix} h_{0,0} & \cdots & h_{0,r_s} \\ \vdots & \ddots & \vdots \\ h_{r_s,0} & \cdots & h_{r_s,r_s} \end{bmatrix} \tag{23}$$

Based on the system's state transition matrix, the steady-state distribution vector $\vec{\lambda}$ of the system's state can then be determined.

$$\vec{\lambda} = [\lambda_0, \lambda_1, \lambda_2, \cdots, \lambda_{r_s}] \tag{24}$$

3.3 Performance Evaluation Metrics

To comprehensively evaluate the performance of SU in cognitive radio networks, particularly their system behavior under different channel allocation protocols, we derive two performance metrics: throughput and packet rejection rate—based on the steady-state distribution vector of the joint system state.

3.3.1 Average Throughput

Throughput is a key metric for measuring a system's capability to successfully transmit data packets within a unit time slot. It is defined as the expected number of packets successfully sent from the buffer during a specific time slot period. In the model established in this paper, throughput not only reflects the data transmission efficiency of the SU within each time slot but also indicates the probability of transmission under different buffer states through a probability distribution.

The probability distribution that the i-th SU transmits a packet within a given time slot is represented as:

$$\vec{\tau}_i = \vec{\lambda} \sum_{k=1}^{\prod_{n=1}^{N} N_{SNR}^n} \varphi_a^k \cdot \min(\xi_i, L_i) \quad \cdot \mathrm{Conv}\left(\vec{\sigma}_{(i,1)}, \vec{\sigma}_{(i,2)}, \vec{\sigma}_{(i,3)}, \cdots, \vec{\sigma}_{(i,N_{SNR}^i)}\right) \tag{25}$$

where $\vec{\tau}_i = [\tau_i^0, \tau_i^1, \tau_i^2, \cdots, \tau_i^{(L_i)}]$ and τ_i^j denotes the probability that the i-th SU transmits j packets in a given time slot.

The average throughput of the i-th SU is denoted as T_{thr}^i:

$$T_{thr}^i = \sum_{j=0}^{L} j \cdot \vec{\tau}_i^{\,j} \tag{26}$$

Here, j represents the number of throughput data packets for the i-th SU.

3.3.2 Average Packet Rejection Rate

The packet rejection rate indicates the average number of packets that are discarded within a single time slot due to insufficient capacity in the SU buffer. It serves as a critical metric for measuring buffer overflow and loss of service quality, directly reflecting the effectiveness of channel allocation strategies in buffer management.

Within a single time slot, the number of packets that may be rejected by the buffer of the i-th SU is denoted as $\vec{e}_i$:

$$\vec{e}_i = \sum_{c=0}^{q_{\max}} \max\left(0, b_i + c - L_i\right) \cdot \vec{p}_j \tag{27}$$

Among these, q_{max} denotes the maximum number of packets arriving within each time slot, b_j represents the current number of packets in the buffer, c indicates the number of newly arriving packets in the current time slot, L_i signifies the total capacity of the SU buffer, and $\vec{p}_j$ describes the probability distribution of arriving packets.

The packet rejection probability distribution for the i-th SU is:

$$\vec{\Lambda}_i = \vec{\lambda} \sum_{k=1}^{\prod_{n=1}^{N} n_{SNR}^{n}} \varphi_a^k \vec{e}_i = \left[\Lambda_i^1, \Lambda_i^1, \Lambda_i^2, \cdots, \Lambda_i^{L_i}\right] \tag{28}$$

Among these, Λ_i^j denotes the probability that the i-th SU rejects j packets within a single time slot.

The average packet rejection rate for the i-th SU is T_{rej}^i:

$$T_{rej}^i = \sum_{j=0}^{L_i} j \cdot \vec{\Lambda}_i^j \tag{29}$$

4 Traffic Pattern-Adaptive Allocation protocol

To further enhance the service performance of SU in cognitive radio networks, this paper proposes an adaptive window allocation protocol. This protocol employs adaptive windows to refine the modeling of SU data arrival processes. Based on this, it dynamically updates the arrival state in channel allocation, thereby maintaining stable and efficient resource allocation performance under varying traffic loads and channel conditions. This section systematically outlines the fundamental principles and implementation process of the TPA protocol.

4.1 Maximum Throughput Allocation Protocol

The Maximum Throughput Allocation (MTA) protocol is a classic resource allocation scheme in CRN where SU schedule PU idle spectrum resources. Its core objective is to maximize the instantaneous data transmission efficiency of the CR system, enabling the resource utilization value of PU idle spectrum to be instantly optimized. Within the MTA protocol, each SU's potential transmission capacity is determined based on the Channel Condition State and AMC mode. By estimating the number of data packets each SU can transmit over its corresponding channel, a potential throughput matrix is constructed for each SU-channel pair. The channel allocation scheme that maximizes the overall throughput is then selected.

4.2 TPA protocol

To ensure the quality of service for SU in CRN and further enhance the overall system throughput, this paper improves and extends the maximum throughput allocation protocol by introducing an adaptive window-based data arrival modeling and channel allocation protocol (TPA). Unlike traditional scheduling methods that rely on fixed arrival models, this protocol dynamically and precisely models the packet arrival process of SUs using multi-scale adaptive windows. It directly incorporates the arrival probability obtained from window fusion into the channel allocation framework, thereby establishing a dynamic probabilistic allocation mechanism capable of real-time adaptation to traffic changes.

The adaptive window mechanism designed in this study achieves precise adaptation through dynamic adjustment. Its core operational process is illustrated in Figure 2.

The algorithm for the TPA protocol is detailed in Algorithm 1.

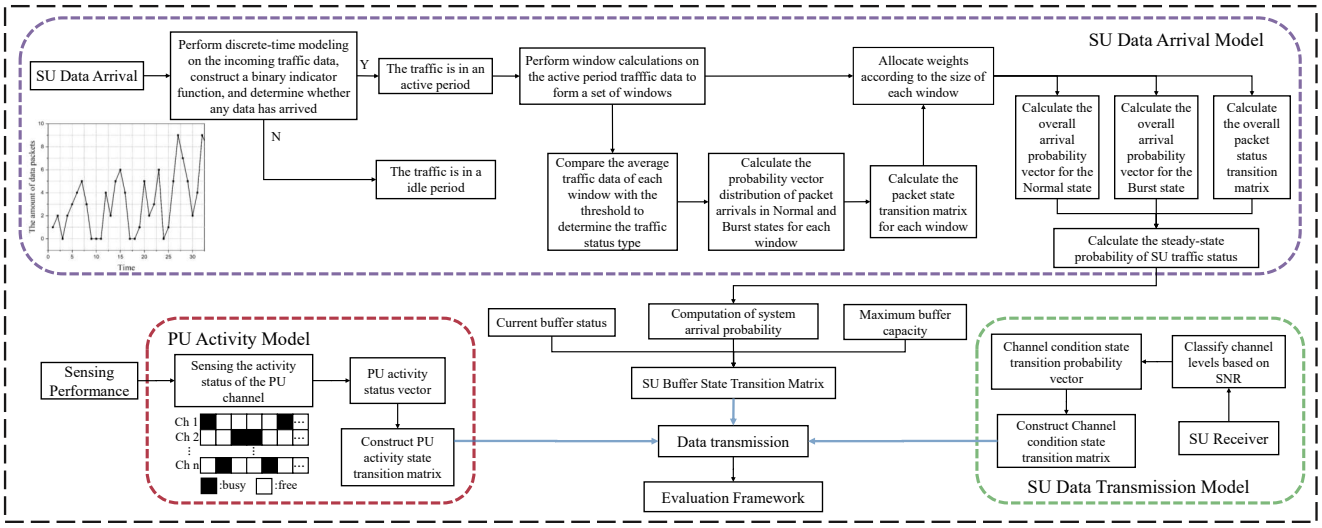

Figure 2. TPA protocol workflow

Algorithm 1 The algorithm of TPA protocol

Input: Number of SUs:M
Number of PU Channels:N
PU activity status:$\vec{s} = (s_1, s_2, , \cdots, s_N)$
SU Buffer status:$\vec{\xi} = (\xi_1, \xi_2, \cdots, \xi_M)$
Channel Condition status:$\vec{\vartheta} = (\vartheta_1, \vartheta_2, \cdots, \vartheta_N)$
Modulation scheme:$\vec{\sigma}_{i,1}, \vec{\sigma}_{i,2}, \vec{\sigma}_{i,3}, \cdots, \vec{\sigma}_{i,N^i_{\mathrm{SNR}}}$
Binary indicator function:X
Window collection:Ω
Window weight:ω
Probability of Normal packet arrival for window i in SU m:$\vec{\sigma}_N^{(m,i)}$
Probability of Burst packet arrival for window i in SU m:$\vec{\sigma}_B^{(m,i)}$
Total probability of Normal packets for SU m:$\vec{p}_N^m$
Total probability of Burst packets for SU m:$\vec{p}_B^m$
State transition matrix of packet arrivals for window i in SU m:$a_{rr}^{(m,i)}$
State transition matrix for SU m's total packet arrivals:A_{rr}^m
Output: $\vec{V}$
Begin:
1: Set $\vec{V} \leftarrow [V_1, V_2, V_3, \cdots, V_{(M+1)^N}]$ $(V_i = 1, \text{for all } i)$
2: Set $X = \{x_t \mid t \in [1, T]\}$
3: Determine whether the traffic is in an idle period or an active period
4: Calculate the length of traffic windows that are in the active period and form a set of windows Ω
5: Set $\Omega \leftarrow \{1, 2, 3, \cdots, n\}$
6: Set $\omega \leftarrow \{\omega_1, \omega_2, \omega_3, \cdots, \omega_i\}$ $(i \in \Omega)$
7: Set $\vec{p}_N^m \leftarrow \sum \omega_i \cdot \vec{\sigma}_N^{(m,i)}$
8: Set $\vec{p}_B^m \leftarrow \sum \omega_i \cdot \vec{\sigma}_B^{(m,i)}$
9: Set $A_{rr}^m \leftarrow \sum \omega_i \cdot a_{rr}^{(m,i)}$
10: Set steady-state probability vector of SU $m \leftarrow \vec{\pi}_m$
11: Set $\vec{\pi}_m \leftarrow \{\pi_N^m, \pi_B^m\}$
12: Set total arrival probability of SU m: $\vec{p}_m$
13: Set $\vec{p}_m \leftarrow \vec{p}_N^m \cdot \pi_N^m + \vec{p}_B^m \cdot \pi_B^m$
14: $\mathbf{V} \leftarrow \mathrm{DAWA}(M, N, \vec{s}, \vec{\xi}, \vec{p}_m)$
15: **return** $\vec{V}$
End

Table 1. Default parameters

Symbol	Meaning	Value
M	Number of SUs	2
N	Number of PU channels	2
L_i	Buffer size	2
$\vec{p}_1$	TPA SU 1 Arrival Probability(Burst Service State)	$[0.05, 0.45, 0.45, 0.05]$
$\vec{p}_2$	TPA SU 2 Arrival Probability(Normal Service State)	$[0.25, 0.25, 0.25, 0.25]$
$\vec{\sigma}_{1,0}$	Modulation scheme of the 1-st SU when channel condition state is 0	$[0.5, 0.5, 0, 0]$
$\vec{\sigma}_{1,1}$	Modulation scheme of the 1-st SU when channel condition state is 1	$[0.1, 0.2, 0.3, 0.4]$
$\vec{\sigma}_{2,0}$	Modulation scheme of the 2-nd SU when channel condition state is 0	$[0.5, 0.5, 0, 0]$
$\vec{\sigma}_{2,1}$	Modulation scheme of the 2-nd SU when channel condition state is 1	$[0.1, 0.2, 0.3, 0.4]$
A_{rr}	Packet Arrival State Transition Matrix	$\begin{bmatrix} 0.9 & 0.1 \\ 0.9 & 0.1 \end{bmatrix}$
P_Θ	Channel State Transition Probability Matrix	$\begin{bmatrix} 0.5 & 0.5 \\ 0.5 & 0.5 \end{bmatrix}$
P_S	Probability Matrix for PU Activity State Transitions	$\begin{bmatrix} 0.2 & 0.8 \\ 0.2 & 0.8 \end{bmatrix}$

5 Numerical Results and Analysis

To evaluate TPA protocol, this paper designs three sets of comparative experiments based on the proposed unified performance analysis framework, conducting a systematic quantitative comparison between the TPA protocol and MTA protocol. These experiments analyze not only the performance of individual SUs but also the overall SU system. They further investigate the impact of SU buffer size, the transition probability matrix of PU activity states, and the transition probability matrix of channel condition states on key SU performance metrics: average throughput and average packet rejection rate.

It should be noted that the proposed framework is formulated based on a joint Markov and queuing-theoretic model, which results in an exponential a growth of the state space with respect to the number of secondary users and primary channels. Consequently, exhaustive numerical simulations under large-scale configurations become computationally prohibitive. Therefore, all simulations are conducted under small-scale settings with $M = N = 2$, which are sufficient to capture the fundamental dynamics of SU–PU interactions and to reveal the performance trends of the proposed protocol.

This experimental system configures two SU and two PU channels. For all configurable variables, a set of baseline parameters is selected to validate the effectiveness of the proposed framework. The specific parameters are shown in Table 1. Although SU1 and SU2 exhibit different arrival probability distributions, they belong to the same class of delay-tolerant, non-real-time users. The difference in arrival probabilities is used to reflect diversity in traffic intensity patterns rather than heterogeneous QoS requirements.

In the adaptive window protocol, the weight of each window is dynamically allocated based on its length relative to the total window length. The average throughput of the i-th SU is calculated as the weighted sum of the throughputs across all windows:

$$T_{thr}^{i} = \sum_{n=1}^{\Omega} \omega_n T_{thr}^{(i,n)} \tag{30}$$

Here, $T_{thr}^{(i,n)}$ denotes the average throughput of the i-th SU in the n-th window, while ω_n represents the weight value of the n-th window. The average packet rejection rate is obtained in the same manner.

Experiment 1 is designed as a buffer-size sensitivity analysis, primarily evaluates the performance of individual SUs by altering their buffer sizes to influence average throughput and average packet rejection rate. SU1 buffer size L_1 ranges from i ($i \in \{2, 3, \cdots, 8\}$) with a step size of 1, while SU2 buffer size L_2 is fixed at 2. This ensures SU1's performance variation stems solely from its buffer size configuration, not inter-SU resource contention. Additionally, the PU activity state transition matrix and channel state transition matrix retain default settings: PU transitions from free to busy state and from busy to busy state have a probability of 0.2, while transitions from free to free state and from busy to free state have a probability of 0.8. This ensures relatively abundant spectrum resources, preventing resource scarcity from masking the impact of buffer size. The transition probability between high-quality and low-quality states for the channel is set to an equal 0.5, eliminating channel quality bias (such as persistent high or low quality) and ensuring that SU1's performance fluctuations are solely related to its own cache.

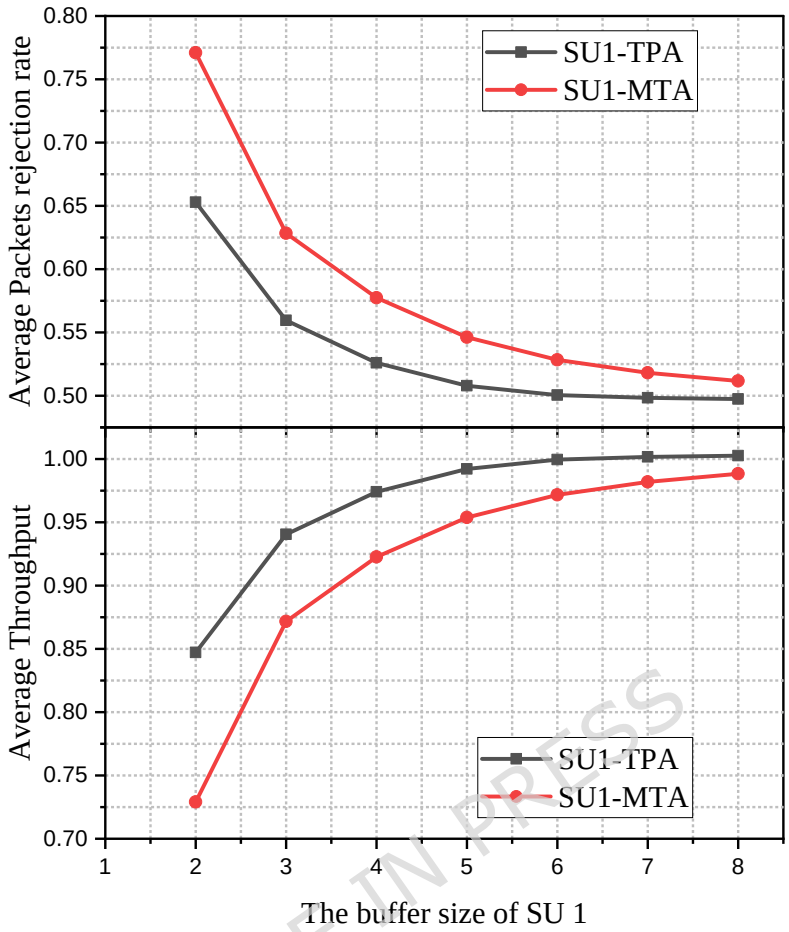

Figure 3. Sensitivity analysis of SU1 performance with respect to buffer size

As buffer capacity increases, the number of packets an SU can accommodate grows, enhancing its traffic handling capability during traffic bursts. This allows the SU to process more valid packets during transmission while reducing packet loss caused by insufficient buffering.

As shown in Figure 3,both the TPA and MTA protocols exhibit an upward trend in throughput as the SU buffer size increases, while the packet rejection rate continues to decrease. However, the TPA protocol consistently achieves higher throughput than the MTA protocol. When the buffer size is 1, TPA's throughput is approximately 0.85, while MTA's is about 0.75. When the buffer size increases to 8, TPA approaches 1.0, and MTA reaches approximately 0.98, demonstrating TPA's superior adaptability to enhanced caching resources. Furthermore, the packet rejection rate of the TPA protocol consistently remained lower than that of the MTA protocol. For instance, with a buffer size of 1, TPA recorded approximately 0.65 while MTA reached 0.77. When the buffer size increased to 8, TPA decreased to 0.50, and MTA remained around 0.52. This reflects TPA's ability to dynamically adjust window weights, enabling more precise matching of cache capacity and reducing packet loss caused by cache overflow.

Experiment 2 primarily investigates the impact of dynamic changes in PU activity states on the overall performance of the SU system. Its core variable is the PU activity state transition probability matrix:

$$P_S = \begin{bmatrix} j & 1-j \\ j & 1-j \end{bmatrix} \quad (j \in \{0.2, 0.3, \cdots, 0.9\}) \tag{31}$$

The value step for j is 0.1, where j represents the probability of a PU switching from its current state (Busy/Free) to the busy state. Additionally, the SU buffer sizes (L_1,L_2) are both fixed at 2, and the values in the channel state transition probability matrix P_Θ are uniformly set to 0.5. This ensures that variations in system performance are solely determined by the PU spectrum resource supply, rather than being influenced by the SU's own resource constraints or channel quality interference.

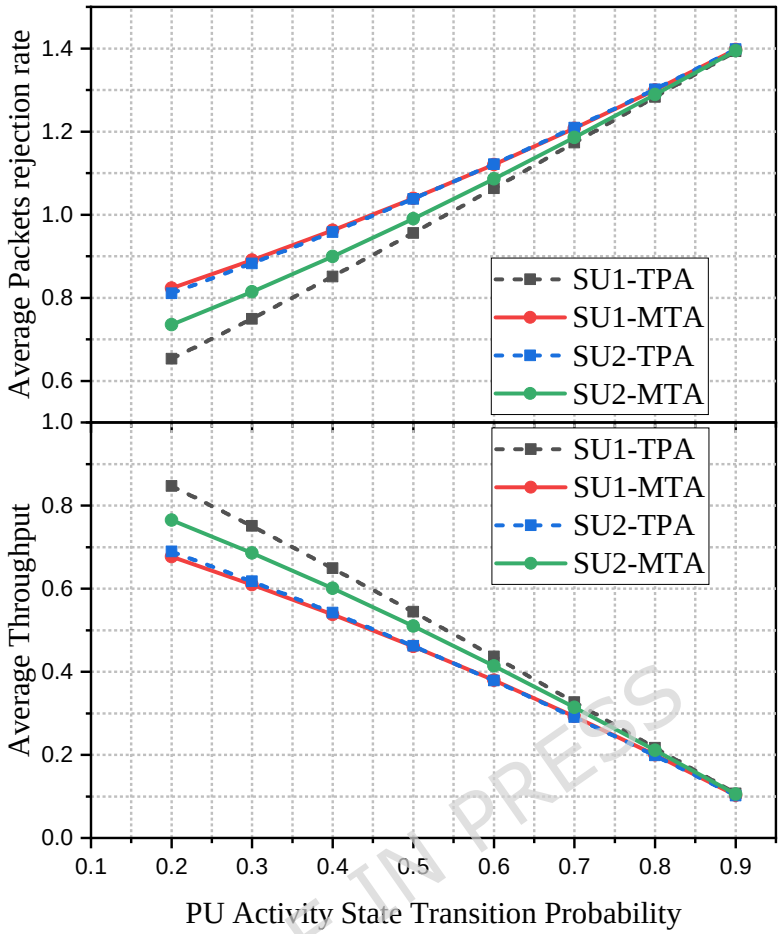

Figure 4. Impact of PU activity state transition probability variations on SU system performance

As the transition probability of the PU activity state increases, PUs occupy available channels more frequently. Under these conditions, the idle spectrum resources available to SUs are significantly reduced, leading to fewer effective transmission slots. Consequently, the number of packets successfully transmitted per unit time decreases. Simultaneously, the higher probability of channel occupation by PUs limits SU access opportunities. During burst traffic conditions, packets accumulated in the queue are forced to be discarded due to prolonged inability to obtain channel access, resulting in a sustained increase in packet rejection rates.

As shown in the experimental results of Figure 4: When the PU state transition probability increases, both the TPA protocol and the MTA protocol exhibit a noticeable decline in the average throughput of the SU, while the packet rejection rate simultaneously rises. However, the two protocols exhibit significant differences in the rate of performance degradation and environmental adaptability. Across the entire range of transition probabilities, the TPA protocol consistently outperforms MTA, demonstrating superior adaptability to changes in PU activity. It achieves higher individual throughput and lower packet rejection rates for SUs under varying levels of spectrum resource availability.

Experiment 3 primarily analyzes the impact of channel quality fluctuation characteristics on the overall performance of the SU system, with the channel state transition probability matrix serving as its core variable:

$$P_{\Theta} = \begin{bmatrix} j & 1-j \\ j & 1-j \end{bmatrix} \quad (j \in \{0.2, 0.3, \cdots, 0.8\}) \tag{32}$$

The value step for j is 0.1, where j represents the probability of the channel transitioning from its current state to a low-quality state. Additionally, the SU buffer sizes (L_1,L_2) are both fixed at 2 to eliminate the influence of individual SU caching resources, ensuring that system performance variations are solely determined by channel quality dynamics. The PU activity state transition probability matrix retains its default settings:

$$P_S = \begin{bmatrix} 0.2 & 0.8 \\ 0.2 & 0.8 \end{bmatrix}$$

By maintaining the stability of the PU idle probability, spectrum resources are kept at an ample level, avoiding the dual interference of resource scarcity and channel fluctuations. This ensures that variations in system performance correspond directly to fluctuations in channel quality.

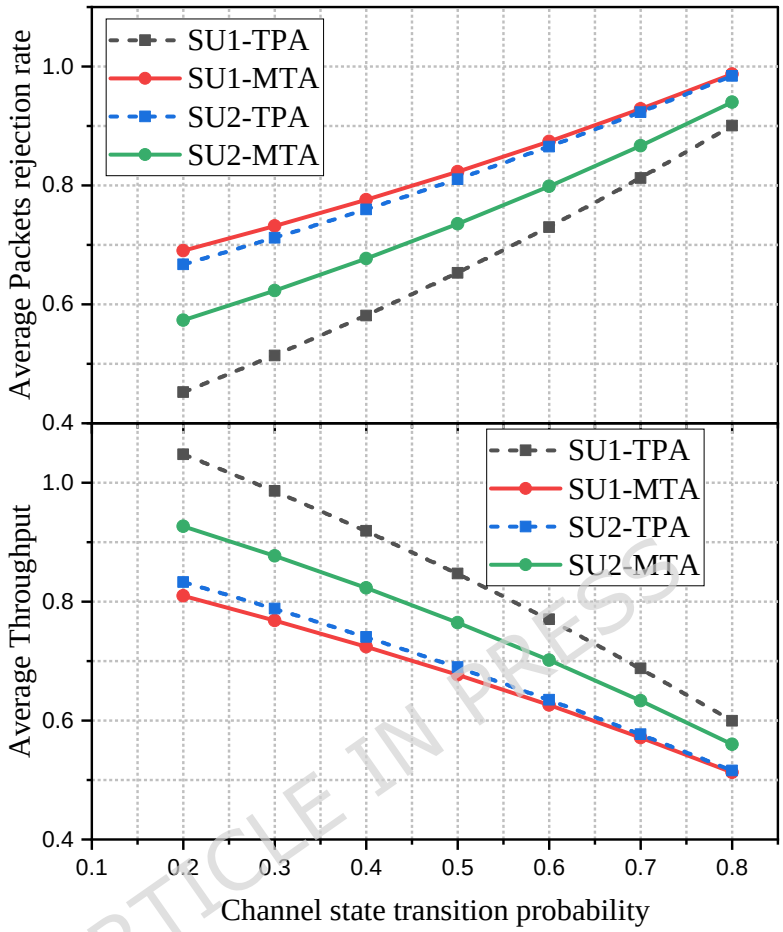

Figure 5. Impact of channel state transition probability variations on SU system performance

As the probability of channel state transitions increases, the channel switches more frequently from high-quality to low-quality states, causing the SU's average transmission rate to steadily decline. Since low-quality channels correspond to higher error rates, a large number of packets require retransmission, further occupying buffer resources and reducing the data space available for normal operations. When accumulated retransmissions lead to persistent buffer overflow, packets are forcibly discarded due to buffer overflow or retransmission timeouts.

As shown in the results of Figure 5, for both SU1 and SU2, the throughput under the TPA protocol consistently outperforms that of the MTA protocol as the channel state transition probability increases, while its packet rejection rate remains lower than that of MTA. This demonstrates that TPA more effectively captures the time-varying characteristics of channel quality and enhances resource utilization efficiency through adaptive window adjustment, thereby maintaining superior SU performance under complex channel conditions.

6 Conclusion and Future Work

This study addresses the complexity of characterizing time-varying SU data arrival in multi-channel Cognitive Radio Networks. We propose an TPA protocol, underpinned by a Markovian queuing framework, which dynamically adjusts window weights to accurately model arrival patterns. Our unified evaluation framework quantifies key performance indicators, including average throughput and packet rejection rates, for both individual users and the system as a whole.

Comparative simulations against the benchmark MTA protocol—considering variables such as SU cache capacity, Primary User activity, and channel quality—demonstrate that the TPA protocol achieves significantly higher throughput and lower

packet rejection rates, exhibiting superior adaptability to dynamic traffic.

In this work, all secondary users are modeled as homogeneous, delay-tolerant, non-real-time users, which allows the proposed framework to focus on accurate traffic modeling and closed-form performance evaluation. Extending the current framework to support heterogeneous SU traffic with differentiated delay requirements, such as real-time and non-real-time services, can be considered as a potential direction for future research.

While the proposed framework enables fine-grained traffic characterization and analytical tractability, its computational complexity grows exponentially with the number of PU channels and SUs due to the expansion of the joint state space. This complexity represents an inherent trade-off between modeling accuracy and scalability. Accordingly, developing scalable solutions, including parallel or distributed computation techniques, state-space reduction strategies,and low-complexity approximation models which can considered a future direction for research.

References

1. Nasser, A., Al Haj Hassan, H., Abou Chaaya, J., Mansour, A. & Yao, K.-C. Spectrum sensing for cognitive radio: Recent advances and future challenge. *Sensors* **21**, 2408 (2021).
2. Muzaffar, M. U. & Sharqi, R. A review of spectrum sensing in modern cognitive radio networks. *Telecommun. Syst.* **85**, 347–363 (2024).
3. Khalek, N. A., Tashman, D. H. & Hamouda, W. Advances in machine learning-driven cognitive radio for wireless networks: A survey. *IEEE Commun. Surv. & Tutorials* **26**, 1201–1237 (2023).
4. Wang, X., Teraki, Y., Umehira, M., Zhou, H. & Ji, Y. A usage aware dynamic spectrum access scheme for interweave cognitive radio network by exploiting deep reinforcement learning. *Sensors* **22**, 6949 (2022).
5. Cullen, A. C., Rubinstein, B. I., Kandeepan, S., Flower, B. & Leong, P. H. Predicting dynamic spectrum allocation: a review covering simulation, modelling, and prediction. *Artif. Intell. Rev.* **56**, 10921–10959 (2023).
6. Zaheer, O., Ali, M., Imran, M., Zubair, H. & Naeem, M. Efficient resource allocation for 5g/6g cognitive radio networks using probabilistic interference models. *Phys. Commun.* **64**, 102335 (2024).
7. Mitola, J. & Maguire, G. Q. Cognitive radio: making software radios more personal. *IEEE personal communications* **6**, 13–18 (2002).
8. Muzaffar, M. U. & Sharqi, R. A review of spectrum sensing in modern cognitive radio networks. *Telecommun. Syst.* **85**, 347–363 (2024).
9. Zaheer, O., Ali, M., Imran, M., Zubair, H. & Naeem, M. Efficient resource allocation for 5g/6g cognitive radio networks using probabilistic interference models. *Phys. Commun.* **64**, 102335 (2024).
10. Luo, S. & Chen, Z. Mode-aware radio resource allocation algorithm in hybrid users based cognitive radio networks. *Sensors* **25**, 5086 (2025).
11. Li, Z.-q., Liu, X. & Ning, Z.-l. Dynamic spectrum access based on deep reinforcement learning for multiple access in cognitive radio. *Phys. Commun.* **54**, 101845 (2022).
12. Giri, M. K. & Majumder, S. Distributed dynamic spectrum access through multi-agent deep recurrent q-learning in cognitive radio network. *Phys. Commun.* **58**, 102054 (2023).
13. Dong, L., Qian, Y. & Xing, Y. Dynamic spectrum access and sharing through actor-critic deep reinforcement learning. *EURASIP J. on Wirel. Commun. Netw.* **2022**, 48 (2022).
14. Liu, X. *et al.* Impacts of sensing energy and data availability on throughput of energy harvesting cognitive radio networks. *IEEE Transactions on Veh. Technol.* **72**, 747–759 (2022).
15. PalunčIć, F., Alfa, A. S., Maharaj, B. T. & Tsimba, H. M. Queueing models for cognitive radio networks: A survey. *IEEE Access* **6**, 50801–50823 (2018).
16. Mehr, K. A., Niya, J. M. & Akar, N. Queue management for two-user cognitive radio with delay-constrained primary user. *Comput. Networks* **142**, 1–12 (2018).
17. Yan, J., Zhang, B., Wang, S., Lan, H. & Wang, X. Burst traffic: Congestion management and performance optimization strategies in heterogeneous cognitive radio networks. *IET Commun.* **18**, 523–533 (2024).
18. Alfa, A. S. *Queueing theory for telecommunications: discrete time modelling of a single node system* (Springer Science & Business Media, 2010).

19. Chakraborty, T., Mukhopadhyay, A., Bhunia, S., Misra, I. S. & Sanyal, S. K. Analysis and enhancement of qos in cognitive radio network for efficient voip performance. In *2011 World Congress on Information and Communication Technologies*, 904–909 (IEEE, 2011).

20. Mehr, K. A., Niya, J. M. & Akar, N. Queue management for two-user cognitive radio with delay-constrained primary user. *Comput. Networks* **142**, 1–12 (2018).

21. Wang, S., Zhang, J. & Tong, L. A characterization of delay performance of cognitive medium access. *IEEE Transactions on Wirel. Commun.* **11**, 800–809 (2012).

22. Adem, N. & Hamdaoui, B. Delay performance modeling and analysis in clustered cognitive radio networks. In *2014 IEEE Global Communications Conference*, 193–198 (IEEE, 2014).

23. Zhao, Q. & Sadler, B. M. A survey of dynamic spectrum access. *IEEE signal processing magazine* **24**, 79–89 (2007).

24. Zhao, Y., Yue, W. & Takahashi, Y. Comparison of a probabilistic returning scheme for preemptive and non-preemptive schemes in cognitive radio networks with two classes of secondary users. *IEICE Transactions on Commun.* **105**, 338–346 (2022).

25. Liu, W., Wang, Y. & Zhang, M. Packet loss rate analysis of cognitive radio mta protocol based on m/m/1 queue. *J. Electron. & Inf. Technol.* **41**, 1987–1993 (2019).

26. Wang, S., Maharaj, B. T. & Alfa, A. S. A maximum throughput channel allocation protocol in multi-channel multi-user cognitive radio network. *J. communications networks* **20**, 111–121 (2018).

27. Vinod, M., Sharma, I. & Singh, G. Throughput maximization based on optimal access probabilities in cognitive radio system. *Int. J. Commun. Syst.* **38**, 1–18 (2025).

28. Alonso, R. M. *et al.* Multi-objective optimization of cognitive radio networks. *Comput. Networks* **184**, 107651 (2021).

29. Jia, J., Zhang, J. & Zhang, Q. Cooperative relay for cognitive radio networks. In *IEEE INFOCOM 2009*, 2304–2312 (IEEE, 2009).

30. Zhao, Q. & Swami, A. A survey of dynamic spectrum access: Signal processing and networking perspectives. In *2007 IEEE International Conference on Acoustics, Speech and Signal Processing-ICASSP'07*, vol. 4, IV–1349 (IEEE, 2007).

31. Li, Y., Wang, H. & Chen, S. Joint state-aware channel allocation for cognitive radio networks: Integrating PU activity, channel quality, and SU buffer dynamics. *IEEE Transactions on Wirel. Commun.* **21**, 7214–7227 (2022).

32. Zhang, X., Liu, Q. & Zhao, W. Traffic-aware dynamic channel allocation for cognitive radio networks under bursty service arrivals. In *Proceedings of the IEEE Global Communications Conference (GLOBECOM)*, 1–6 (2023).

33. Raj, A. & Gupta, R. Multi-dimensional state integration in cognitive radio channel allocation: Mitigating buffer overflows under complex traffic. *IEEE Internet Things J.* **11**, 8231–8242 (2024).

34. Chen, L., Zhou, Y. & Hu, X. Joint pu-su-channel state modeling for dynamic channel allocation in cognitive radio networks. *IEEE Transactions on Cogn. Commun. Netw.* **7**, 1123–1135 (2021).

35. Zhao, Y., Liu, S. & Wang, Q. Deep reinforcement learning for joint state-aware channel allocation under complex traffic in cognitive radio networks. *IEEE Transactions on Wirel. Commun.* **23**, 1245–1258 (2024).

36. Raj, P. & Kumar, V. Multi-state integrated channel allocation for cognitive radio iot networks with bursty service arrivals. *IEEE Wirel. Commun. Lett.* **14**, 521–525 (2025).

37. Liu, H., Zhang, T. & Chen, J. Cross-layer channel allocation integrating pu activity, channel condition and traffic arrival in cognitive radio networks. In *Proceedings of the IEEE Wireless Communications and Networking Conference (WCNC)*, 2101–2106 (2023).

Author contributions statement

M.Z. (Zhang Min) conceived the overall research direction, provided critical supervision and guidance for the project, and revised the manuscript for important intellectual content; Z.W. (Wu Ziru, corresponding author) designed the specific research methodology, led the experimental implementation, analyzed the core data, wrote the main body of the manuscript, and coordinated the revision process; J.B. (Bai Jinyuan) performed supplementary experiments, processed data sets, prepared all figures and tables, and assisted with the drafting of the introduction section; B.Z. (Zhang Bo) conducted the literature review and assisted with experimental validation. All authors reviewed and approved the final version of the manuscript.

Funding

The author received no specific funding for this work

Declaration of Competing Interests

The authors declare no competing interests.

Data availability

The data generated and analyzed in this study are real and were produced by the authors. The datasets used to support the findings of this research are available from the corresponding author upon reasonable request.